Disorder-induced tail states in gapped bilayer graphene

V. V. Mkhitaryan and M. E. Raikh

Department of Physics, University of Utah, Salt Lake City, Utah 84112, USA

The instanton approach to the in-gap fluctuation states is applied to the spectrum of biased bilayer graphene. It is shown that the density of states falls off with energy measured from the band edge as $\nu(\epsilon) \propto \exp(-|\epsilon/\epsilon_t|^{3/2})$, where the characteristic tail energy, ϵ_t, scales with the concentration of impurities, n_i, as $n_i^{2/3}$. While the bare energy spectrum is characterized by two energies: the bias-induced gap, V, and interlayer tunneling, $t_\perp$, the tail, ϵ_t, contains a *single* combination $V^{1/3}t_\perp^{2/3}$. We show that the above expression for $\nu(\epsilon)$ in the tail actually applies all the way down to the midgap.

I. INTRODUCTION

Several experimental studies of electronic properties of graphene bilayers were recently reported in the literature.[1–8] While experiments[1–5] were carried out on unbiased, and thus gapless[9] bilayers, the focus of the papers[6–8] was the fact that a tunable gap emerges in the energy spectrum of bilayer upon applying an interlayer bias.[9,10] Various consequences of the opening of the gap were studied theoretically in Refs. [11–21]. One of these consequences is that biased bilayer responds to disorder as a "normal" semiconductor, i.e., impurities give rise to the tails of the density of states which extend into the gap from the bottom of conduction and from the top of the valence band. Such in-gap localized states are especially relevant to the experiment in Ref. [8], where the inelastic transport over these states has been observed. This raises a theoretical question about the shape of in-gap fluctuation tails in bilayers and their dependence on the disorder strength. Previous papers on biased graphene bilayers with impurities[13] or general diagonal disorder[22] do not study the in-gap fluctuation tails but rather the disorder-induced smearing of the band edges. Also, the numerical results for the density of states are presented in Ref. [13] for particular values of impurity concentration, n_i, so that the general dependence of the magnitude of smearing on n_i, as well as on the interlayer bias, V, was not established.

In the present paper we study analytically the density of disorder-induced localized in-gap states in bilayer graphene. The reason why classical results[23–25] for the fluctuation tails do not directly apply to this situation is a peculiar structure of the bare energy spectrum shown in Fig. 1. In particular, the minimum (maximum) of the electron (hole) dispersion is located at finite momentum,[10] p_0. Also, at energies of the order of the gap, the dispersion law is not quadratic but rather $\epsilon(p) \propto p^4$. These two features naturally define two regimes of disorder-induced broadening of the density of states:

(i) Weak disorder. The magnitude of smearing in this regime is smaller than the depth of the minimum in Fig. 1. As a result, the states responsible for the smearing have momenta close to p_0.[26] This fact, as was pointed out in Ref. [13], facilitates localization of electrons (holes) by weak impurities. Earlier this observation was made in Refs. [27–29].

(ii) Strong disorder. The Mexican-hat structure in Fig. 1 is completely smeared. In this regime, the in-gap states are

formed due to trapping of electrons (holes) with *quartic* dispersion by certain disorder configurations.

Below we demonstrate that in both regimes the magnitude of smearing, ϵ_t, is proportional to the combination $n_i^{2/3}V^{1/3}$. Clearly, for the gap to be resolved, the applied bias must exceed ϵ_t. This suggests that the threshold bias for which $V > \epsilon_t$ is proportional to the first power of n_i. We find the shape of the density of states near the band edges for two regimes by extending the instanton approach of Refs. [23] and [24] to the spectrum of a biased bilayer graphene. We restrict consideration to the case of short-range impurity potential, $w(\mathbf{r})$, so that the correlator of the disorder potential is

$$\langle U(\mathbf{r})U(\mathbf{r}')\rangle = \gamma\delta(\mathbf{r} - \mathbf{r}'), \tag{1}$$

with

$$\gamma = n_i\left[\int d\mathbf{r}w(\mathbf{r})\right]^2. \tag{2}$$

We also assume that the bias is smaller than the interlayer tunneling constant,[9,10] $t_\perp$.

II. BARE DENSITY OF STATES

Due to interlayer hopping, the spectrum of the bilayer graphene becomes parabolic,[9,10] $\epsilon(p) = \pm c^2p^2/t_\perp$, where c is the Dirac velocity in graphene. For "small" momenta, $cp \ll t_\perp$, the gap opens upon applying the bias, V, between the layers. For $V < t_\perp$, the low-energy Hamiltonian of the bilayer graphene can be reduced[11,30] to the 2×2 matrix
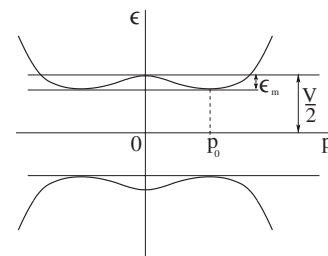

FIG. 1. Energy spectrum of a biased bilayer graphene has a loop of minima of depth ϵ_m [Eq. (10)] at $|\mathbf{p}|=p_0$ [Eq. (6)]. At small bias, $V < t_\perp$, the gap is smaller than the distance to the next subbands.

$$\mathcal{H} = \begin{pmatrix} \dfrac{V}{2}\left(1 - 2\dfrac{c^2 p^2}{t_\perp^2}\right) & -\dfrac{c^2(p_x + i p_y)^2}{t_\perp} \\ -\dfrac{c^2(p_x - i p_y)^2}{t_\perp} & -\dfrac{V}{2}\left(1 - 2\dfrac{c^2 p^2}{t_\perp^2}\right) \end{pmatrix}, \quad (3)$$

which yields the spectrum

$$\epsilon^2(p) = \frac{V^2}{4}\left(1 - 2\frac{c^2 p^2}{t_\perp^2}\right)^2 + \frac{c^4 p^4}{t_\perp^2}. \quad (4)$$

It is seen that in addition to opening the gap, finite bias, V, leads to negative effective mass at small momenta. Disorder affects the energy domains $|\epsilon(p) \pm V/2| \ll V$, close to the band edges. In these domains the spectrum can be further simplified to

$$\epsilon^\pm(p) = \pm\left[\frac{V}{2} + \frac{c^4}{V t_\perp^2}(p^2 - p_0^2)^2\right], \quad (5)$$

where

$$p_0 = \frac{V}{\sqrt{2}\, c} \quad (6)$$

is the minimum position (Fig. 1). In Eq. (5) we also took into account that $V \ll t_\perp$. The eigenfunctions, corresponding to the two branches, have the form

$$\chi_{\mathbf{p}}^+(\mathbf{r}) \approx e^{i\mathbf{p}\mathbf{r}} \begin{pmatrix} e^{2i\phi_{\mathbf{p}}} \\ -\dfrac{c^2 p^2}{V t_\perp} \end{pmatrix}, \quad \chi_{\mathbf{p}}^-(\mathbf{r}) \approx e^{i\mathbf{p}\mathbf{r}} \begin{pmatrix} \dfrac{c^2 p^2}{V t_\perp} \\ e^{-2i\phi_{\mathbf{p}}} \end{pmatrix}, \quad (7)$$

where $\phi_{\mathbf{p}} = \tan^{-1}(p_y/p_x)$ is the azimuthal angle of the vector $\mathbf{p}$. The minimal energy for the branch $\epsilon^+(p)$ is

$$\Delta = \frac{V}{2} - \frac{V^3}{4 t_\perp^2}. \quad (8)$$

Shifting the energy scale origin to Δ, for the bare density of states,[15] $\nu_0(\epsilon)$, we will have

$$\nu_0(\epsilon) = \left(\frac{2 t_\perp^2}{V c^2}\right) \tilde{\nu}\left(\frac{\epsilon}{\epsilon_m}\right), \quad (9)$$

where

$$\epsilon_m = \frac{V^3}{4 t_\perp^2}, \quad (10)$$

is the depth of the minimum (Fig. 1) and the dimensionless function $\tilde{\nu}(z)$ is defined as

$$\tilde{\nu}(z) = \begin{cases} \dfrac{1}{\sqrt{z}}, & 0 < z < 1 \\ \dfrac{1}{2\sqrt{z}}, & z > 1 \end{cases}. \quad (11)$$

Equation (11) applies up to $z \sim (t_\perp/V)^2$, which corresponds to $\epsilon \sim V$. For higher energies the falloff of $\tilde{\nu}(\epsilon)$ saturates and eventually crosses over to a linear growth, as in the single-layer graphene. Single-scale behavior of $\tilde{\nu}(z)$ ensures that the magnitude of disorder-induced smearing of the band edges is

defined by a single parameter for both weak-disorder and strong-disorder regimes.

III. WEAK DISORDER

In the vicinity of the minimum at $p = p_0$, the dispersion law simplifies[13,15,19] to

$$\epsilon^\pm(\mathbf{p}) = \pm\frac{(|\mathbf{p}| - p_0)^2}{2m}, \quad m = \frac{t_\perp^2}{4 V c^2}. \quad (12)$$

This expansion applies in the domain, $(|\mathbf{p}| - p_0) \ll V/c$, where $\epsilon(\mathbf{p}) - \epsilon(p_0)$ is smaller than the energy distance $V^3/4 t^2$ between the minimum and maximum in Fig. 1. The eigenfunctions of Eq. (7) simplify to

$$\chi_{\mathbf{p}}^+(\mathbf{r}) \approx e^{i\mathbf{p}\mathbf{r}} \begin{pmatrix} e^{2i\phi_{\mathbf{p}}} \\ -\dfrac{V}{2 t_\perp} \end{pmatrix}, \quad \chi_{\mathbf{p}}^-(\mathbf{r}) \approx e^{i\mathbf{p}\mathbf{r}} \begin{pmatrix} \dfrac{V}{2 t_\perp} \\ e^{-2i\phi_{\mathbf{p}}} \end{pmatrix}. \quad (13)$$

One-dimensional character of the spectrum is reflected in the $\epsilon^{-1/2}$ behavior of the density of states Eq. (9) near the band edge. The magnitude, ϵ_t, of disorder-induced broadening can be estimated from the following reasoning. The inverse scattering rate due to the disorder, calculated from the golden rule, is given by

$$\frac{1}{\tau(\epsilon)} = \frac{\gamma}{\pi}\nu_0(\epsilon) = \frac{\gamma t_\perp V^{1/2}}{\pi c^2 \epsilon^{1/2}}. \quad (14)$$

Then the estimate for ϵ_t emerges upon equating $1/\tau(\epsilon_t)$ to ϵ_t, yielding

$$\epsilon_t = \left(\frac{V^{1/2} t_\perp}{c^2}\gamma\right)^{2/3}. \quad (15)$$

Note that the above consideration equally applies for weak disorder, $\epsilon_t < \epsilon_m$, and strong disorder, $\epsilon_t > \epsilon_m$. As follows from Eq. (15), the weak-disorder regime realizes for

$$\gamma \ll c^2\left(\frac{V}{t_\perp}\right)^4. \quad (16)$$

The fact that the fluctuation states in weak-disorder regime are composed essentially from the free states with momenta, p, close to p_0, allows us to obtain an asymptotically exact solution for the density of states in this regime. This was demonstrated in Ref. 28, where the spectrum Eq. (12) emerged as a result of the spin-orbit coupling. The difference between the wave functions [Eq. (13)] and spin-orbit wave functions affects only numerical factors in the final result. Still, for completeness, we will briefly sketch the calculation from Ref. 28 using our notations.

A drastic simplification coming from the condition $\epsilon_t \ll \epsilon_m$ is that the interference between two scattering amplitudes $\mathbf{p} \to \mathbf{p}'$ and $\mathbf{p} \to \mathbf{p}_1 \to \mathbf{p}_2 \to \mathbf{p}'$ is suppressed. This is because the momenta $\mathbf{p}$, $\mathbf{p}_1$, and $\mathbf{p}_2$, which are close to p_0 in *absolute value*, are restricted in their mutual directions by the condition $(|\mathbf{p}_1 + \mathbf{p}_2 - \mathbf{p}| - p_0) \sim p_0(\epsilon_t/\epsilon_m)^{1/2}$. This condition limits the angles between the momenta to $(\epsilon_t/\epsilon_m)^{1/2}$. As a result, the non-random-phase-approximation (non-RPA) dia-

grams in the self-energy, $\Sigma_{\mathbf{p}}(\epsilon)$, are parametrically, in $(\epsilon_t/\epsilon_m)^{1/2}$, smaller than the corresponding random-phase-approximation (RPA) diagrams. In other words, the RPA becomes asymptotically exact in weak-disorder regime.

Within the RPA, the density of states is given by

$$\nu(\epsilon) = \frac{1}{\pi}\mathrm{Im}\sum_{\mathbf{p}} \frac{|\chi_{\mathbf{p}}^{(+)}|^2}{\epsilon - \epsilon(\mathbf{p}) - \sum_{\mathbf{p}}(\epsilon)}, \qquad (17)$$

where the electron self-energy satisfies

$$\mathrm{Im}\sum_{\mathbf{p}}(E) = \gamma\,\mathrm{Im}\int \frac{d\mathbf{p}_1}{(2\pi)^2} \frac{|(\chi_{\mathbf{p}}^{*(+)}\chi_{\mathbf{p}_1}^{(+)})|^2}{E - \epsilon(\mathbf{p}_1) - \sum_{\mathbf{p}_1}(E)}. \quad (18)$$

The fact that $\mathrm{Im}\Sigma_{\mathbf{p}}$ does not depend on $\mathbf{p}$ allows us to express the solution of Eq. (18) in the form,

$$\mathrm{Im}\sum(\epsilon) = \frac{\epsilon_t}{2^{5/3}}A\!\left(\frac{2^{5/3}\epsilon}{\epsilon_t}\right), \qquad (19)$$

where the energy ϵ is defined as

$$\epsilon = E - \left(\frac{V}{2} - \frac{V^3}{4t_\perp^2} + \mathrm{Re}\sum\right), \qquad (20)$$

and the dimensionless function $A(x)$ satisfies the algebraic equation,

$$A(x) = \sqrt{\frac{x + \sqrt{A(x)^2 + x^2}}{A(x)^2 + x^2}}. \qquad (21)$$

The solution of this equation has the form,

$$A(x) = \left(\left[\frac{3^{1/2}2^{1/3}(3^{3/2} + \sqrt{27 + 4x^3})^{1/3}}{(3^{3/2} + \sqrt{27 + 4x^3})^{2/3} - 2^{2/3}x}\right]^2 - x^2\right)^{1/2}. \quad (22)$$

The densities of states per spin and per valley can be expressed via $A(x)$ as

$$\nu(\epsilon) = \frac{1}{\pi\gamma}\mathrm{Im}\sum(\epsilon) = \frac{1}{2^{5/3}\pi}\frac{V^{1/2}t_\perp}{\epsilon_t^{1/2}c^2}A\!\left(\frac{2^{5/3}\epsilon}{\epsilon_t}\right). \quad (23)$$

It is plotted in Fig. 2 together with the bare density of states.

Sharp low boundary of $\nu(\epsilon)$ in Fig. 2 is an artifact of the RPA. In reality it is smeared within the energy interval,

$$\widetilde{\epsilon}_t = \frac{\epsilon_t^{3/2}}{\epsilon_m^{1/2}} = \frac{2\gamma t_\perp^2}{Vc^2} \ll \epsilon_t, \qquad (24)$$

which is much smaller than ϵ_t. This smearing comes from non-RPA diagrams. Concerning the deep tail of $\nu(\epsilon)$, it is close to a simple exponent, namely,

$$\nu(\epsilon) \propto \exp\!\left[-\frac{4|\epsilon|}{\widetilde{\epsilon}_t\,\ln\!\left(\frac{\epsilon_m}{|\epsilon|}\right)}\right]. \qquad (25)$$

The reason why this tail can be found analytically is again the fact that the wave functions of the fluctuation states have two spatial scales; they oscillate rapidly with period p_0^{-1} and decay at much larger distances as $\exp(-\sqrt{2m|\epsilon|}\,r)$. The tail states are very similar to those found in Ref. 28. The key
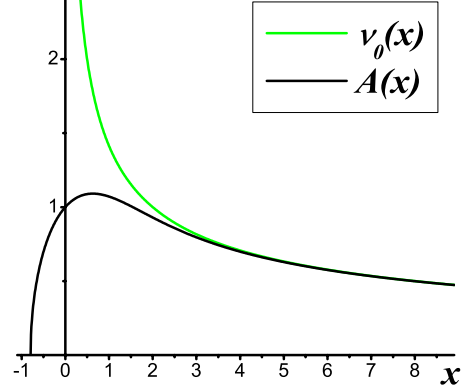

FIG. 2. (Color online) Dimensionless density of states near the band edge is plotted from Eq. (22) versus dimensionless energy $x = \epsilon/\epsilon_t$. Green (gray) line is the high-energy asymptote, $\nu_0(x) = (2/x)^{1/2}$.

steps of derivation of Eq. (25) are outlined in the Appendix.

IV. STRONG DISORDER

We now turn to the case of a strong disorder when $\epsilon_t > \epsilon_m$. The shape of the tail density of states in this case can be established from the following qualitative consideration. The probability density to find a fluctuation $U(\mathbf{r})$ is given by

$$\mathcal{P}\{U(\mathbf{r})\} = \exp\!\left[-\frac{1}{2\gamma}\int d\mathbf{r}\,U^2(\mathbf{r})\right]. \qquad (26)$$

In order to create a localized level with binding energy, ϵ, the magnitude of the fluctuation must exceed $|\epsilon|$, while the size cannot be smaller than the de Broglie wavelength, r_ϵ, of a free electron with energy, ϵ, i.e.,

$$r_\epsilon = \frac{1}{p_\epsilon} = \left(\frac{c^4}{Vt_\perp^2|\epsilon|}\right)^{1/4}, \qquad (27)$$

where the last identity follows from the dispersion law $\epsilon(p) = c^4 p^4/Vt_\perp^2$. Now the integral $\int d\mathbf{r}\,U^2(\mathbf{r})$ can be estimated as $\epsilon^2 r_\epsilon^2$. Substituting this estimate into Eq. (26) and using Eq. (27), we get

$$\nu(\epsilon) \propto \exp\!\left(-\left|\frac{\epsilon}{\epsilon_t}\right|^{3/2}\right). \qquad (28)$$

The remaining task is to establish the numerical coefficient in the exponent [Eq. (28)] with the help of the instanton approach.[23–25] Within this approach, one should solve the Schrödinger equation with potential, $U(\mathbf{r})$, which yields an eigenvalue, E (here we measure energy from the gap center). Then $U(\mathbf{r})$ is determined from the condition that $\int d\mathbf{r}\,U^2(\mathbf{r})$ in the exponent of Eq. (26) is minimal. This restriction is conventionally incorporated by adding to $\int d\mathbf{r}\,U^2(\mathbf{r})$ the energy, $E[\Psi] = \langle\Psi|(\mathcal{H}+U)|\Psi\rangle$, with Lagrange multiplier, λ. Then minimization of

$$\lambda\langle\Psi|(\mathcal{H}+U)|\Psi\rangle - \int d\mathbf{r}\,U^2(\mathbf{r}) \qquad (29)$$

with respect to U yields $U = -\frac{\lambda}{2}|\Psi|^2$.

At this point the following remark is in order. Conventionally, upon substituting the found $U(\mathbf{r})$ back into the Schrödinger equation, the sign of λ is chosen from the condition that potential $U(\mathbf{r})$ is attractive. However, in our case of two symmetric bands, Fig. 1, the potential which is attractive for electrons is repulsive for holes and vice versa. It turns out that choosing $\lambda = 2$ corresponds to $\nu(E)$ which falls off from $E = V/2$ *all the way* down to $E = -V/2$. Correspondingly, choosing $\lambda = -2$ leads to the tail $\nu(-E)$ which grows from $E = -V/2$ toward the bottom of conduction band $E = V/2$. Therefore, at $E = 0$, we have two *different* solutions, with $U(\mathbf{r})$ and $-U(\mathbf{r})$, for which the "electron" and "hole" components of eigenfunction Ψ are related as $(\psi_e, \psi_h) \leftrightarrow (-\psi_h^*, \psi_e^*)$. Thus, in view of exponential character of $\nu(E)$, it is sufficient to set $\lambda = 2$ and consider only positive energies, $E > 0$. The nonlinear instanton equation reads

$$\frac{V}{2}\psi_e - \frac{c^2}{t_\perp}(\partial_x + i\partial_y)^2\psi_h - \psi_e(|\psi_e|^2 + |\psi_h|^2) = E\psi_e,$$

$$-\frac{V}{2}\psi_h - \frac{c^2}{t_\perp}(\partial_x - i\partial_y)^2\psi_e - \psi_h(|\psi_e|^2 + |\psi_h|^2) = E\psi_h. \quad (30)$$

Then, with exponential accuracy, we have $\nu(E) \propto \mathcal{P}\{U(\mathbf{r})\}$, where

$$\mathcal{P}\{U(\mathbf{r})\} = \exp\left[-\frac{1}{2\gamma}\int d\mathbf{r}\, U^2(\mathbf{r})\right]$$

$$= \exp\left[-\frac{1}{2\gamma}\int d\mathbf{r}(|\psi_e|^2 + |\psi_h|^2)^2\right] \quad (31)$$

is the probability of realization of $U(\mathbf{r})$.

Consider first the energies close to the bottom of the conduction band, $-\epsilon = (\frac{V}{2} - E) \ll V$. In this limit, the second equation in the system [Eq. (30)] can be simplified as

$$\psi_h = -\frac{c^2}{Vt_\perp}(\partial_x - i\partial_y)^2\psi_e. \quad (32)$$

Substituting Eq. (32) into the first equation [Eq. (30)] and performing rescaling,

$$r = c(Vt_\perp^2|\epsilon|)^{-1/4}\rho, \quad \psi_e = \left|\frac{\epsilon}{\lambda}\right|^{1/2}f(\rho), \quad (33)$$

we arrive at the following dimensionless instanton equation:

$$\Delta_\rho^2 f(\rho) + f(\rho) - f(\rho)^3 = 0, \quad (34)$$

while the expression for $\nu(\epsilon)$ takes the form,

$$\nu(\epsilon) \propto \exp\left[-\frac{I_4}{2}\left|\frac{\epsilon}{\epsilon_t}\right|^{3/2}\right], \quad (35)$$

where ϵ_t is defined by Eq. (15) and $I_4 = \int d\rho f^4(\rho)$.

Equation (30) has solutions for arbitrary angular momentum, M. However, leading contribution to the density of states comes from azimuthally symmetric solution, $f(\rho)$. Then the hole component [Eq. (32)] of the wave function corresponds to the momentum $\mathcal{M} = 2$, namely,
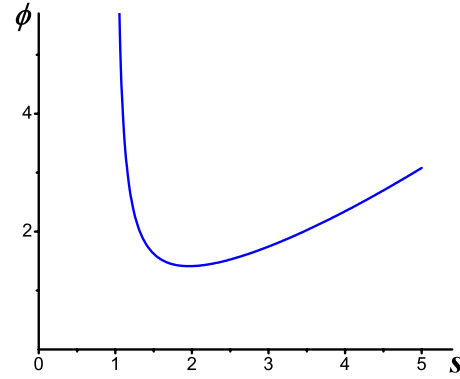

FIG. 3. (Color online) The function $\phi(s)$ is plotted from Eq. (38).

$$\psi_h = \frac{\epsilon}{\sqrt{V\lambda}}e^{-2i\phi}\left(\partial_\rho^2 - \frac{1}{\rho}\partial_\rho\right)f(\rho). \quad (36)$$

A peculiar feature of the nonlinear equation [Eq. (34)] is that it contains Δ_ρ^2 instead of a usual Laplace operator, Δ_ρ. This is a direct consequence of the dispersion law $\epsilon(p) \propto p^4$. As a result, the average "kinetic" energy, $J_2 = \int d\rho[\Delta_\rho f(\rho)]^2$, "potential" energy I_4, and the integral $I_2 = \int d\rho[f(\rho)]^2$ are related as 1:4:3, unlike the relation 1:2:3 for conventional polaron.[31] We solve Eq. (34) by employing the variational approach on the class of trial functions $f(\rho) = C\exp[-(\rho/\rho_0)^s]$. Minimization of the corresponding functional,

$$\Phi\{f\} = \int d\rho\left[(\Delta_\rho f)^2 + f^2 - \frac{1}{2}f^4\right], \quad (37)$$

with respect to C and ρ_0 can be easily performed analytically. The resulting s dependence of $\Phi\{f\}$ has the form,

$$\phi(s) = \left[\pi\frac{s(s-1)+2}{2^{3-4/s}}\frac{\left(1 - \frac{2}{s}\right)}{\sin\pi\left(1 - \frac{2}{s}\right)}\right]^{1/2}. \quad (38)$$

This combination has a well-pronounced minimum at $s \approx 1.963$ (see Fig. 3). On the other hand, the hole wave function Eq. (36) is nonsingular at $\rho \to 0$ if $s \geq 2$. Thus it is reasonable to adopt $s = 2$, yielding $C = 1.63$ and $\rho_0 = 2.21$. This allows us to specify the numerical factor in the exponent of density of states in Eq. (35), namely, $I_4 = 27.36$.

The result [Eq. (35)] applies for $\epsilon_t \ll \epsilon \ll V$. A relevant question for inelastic transport is the density of states at the gap center. For qualitative estimate it is sufficient to substitute $\epsilon = -V/2$ into Eq. (35). To establish the numerical coefficient in the exponent more accurately, we found variational solution of the system [Eq. (30)] for $E = 0$ (Fig. 4). It turns out that the coefficients C and ρ_0 in $f(\rho)$ assume the values 1.6 and 1.96, respectively, and the numerical coefficient in Eq. (35) is $I_4 = 23.22$. We conclude that expression (35) for the tail of the density of states is essentially valid down to the gap center.
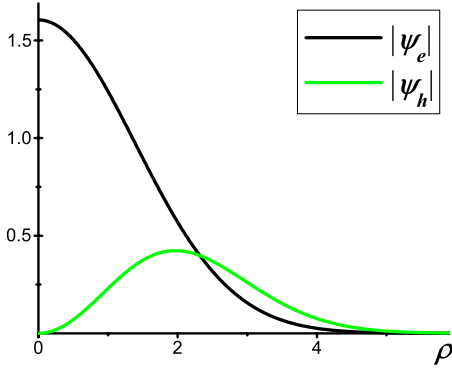
FIG. 4. (Color online) Electron and hole components of the wave function, obtained from variational solution of Eq. (30) for $E=0$, are plotted versus dimensionless distance, ρ, defined by Eq. (33).

V. CONCLUDING REMARKS

Prefactor. Equation (35) describes the tail of the density of states with exponential accuracy. To restore the dimensionality, it is natural to multiply Eq. (35) by $\nu_0(\epsilon_t)$ since the smearing of the band edge is $\sim \epsilon_t$. However, since Eq. (35) describes the deep tail, the prefactor contains an additional power of a dimensionless ratio ($|\epsilon|/\epsilon_t$). To establish this power, one has to follow the procedure of calculating the prefactor in the functional integral.[32,33] Within this procedure, the origin of a prefactor is the fact that the center of the instanton can be shifted in the plane along both axes. These shifts correspond to the so-called zero modes. Each zero mode contributes a factor $(|\epsilon|/\epsilon_t)^{1/4}$. The power 1/4 reflects the size of the instanton fluctuation, $r_\epsilon \propto |\epsilon|^{-1/4}$ [see Eq. (27)]. Overall, within a numerical coefficient, the final expression for the density of states in the tail reads

$$\nu(\epsilon) = \frac{V^{1/2} t_\perp}{c^2 \epsilon_t} |\epsilon|^{1/2} \exp\left[-11.6 \left| \frac{\epsilon}{\epsilon_t} \right|^{3/2} \right]. \quad (39)$$

Note that, unlike the case of parabolic spectrum,[32] for $\epsilon(p) \propto p^4$, the prefactor does not diverge. This is because the second-order shift of the band edge $\propto \gamma \int d\epsilon \nu_0(\epsilon)/\epsilon$ converges at large ϵ for $\nu_0(\epsilon) \propto \epsilon^{-1/2}$.

Relation to the scattering time. Short-range disorder is characterized by a single parameter, γ. For comparison with experiment, this parameter can be related to electron-scattering time, τ_F, in the case when the gate voltage places the Fermi level, E_F, well above the smearing, ϵ_t, of the band edge. Expressing γ from Eq. (14) and substituting into Eq. (15), we obtain

$$\epsilon_t = \left(\frac{4\pi^2 E_F}{\tau_F^2} \right)^{1/3} = \left(\frac{4\pi^4 n_e^2 c^4}{V t_\perp^2 \tau_F^2} \right)^{1/3}. \quad (40)$$

In the second identity we had expressed E_F via electron density, n_e.

The role of intervalley scattering. Our assumption that disorder is short ranged requires that the radius of the impurity potential, $w(r)$, is smaller than the wavelength of electron with energy $\sim V$, which is $\sim c/(Vt_\perp)^{1/2}$. This length is much larger than the lattice constant, and we neglected the

intervalley scattering. If the radius of $w(r)$ is comparable to the lattice constant, the intervalley scattering becomes as efficient as intravalley scattering. This would not only lift the valley degeneracy of the fluctuation states but also result in their azimuthal asymmetry, much similar in the case of degenerate valence band considered in Ref. 34. The consequence of this asymmetry is the change in the numerical factor in the exponent of Eq. (35).

Dependence on impurity concentration. Our main result [Eq. (39)] applies in the limit of strong disorder when $\gamma > c^2 (V/t_\perp)^4$. On the other hand, we assumed that the gap is not washed out completely by the disorder. Then the upper limit on γ can be found by setting $\epsilon = V/2$ in Eq. (39) equating the exponent to 1. Finally, it is convenient to present the domain of validity of Eq. (39) as

$$\left(\frac{V}{t_\perp} \right)^4 < \frac{\gamma}{c^2} < 4.1 \frac{V}{t_\perp}. \quad (41)$$

It follows from the second condition that the minimal $V = V_c$, at which the gap effectively opens, is proportional to the impurity concentration, as it was stated in Sec. I. We can also rewrite the above condition in terms of dimensionless conductance when the Fermi level is in the conduction band,

$$E_F \tau_F > 1.5 \left(\frac{E_F}{V} \right)^{3/2}. \quad (42)$$

Finally, we address the case of low impurity concentration when the first condition [Eq. (41)] is violated.

An isolated impurity with potential, $w(r)$, creates a localized state with binding energy,[27–29]

$$\epsilon_b = 2\pi^2 m p_0^2 \left[\int d\mathbf{r} w(r) J_0^2(p_0 r) \right]^2. \quad (43)$$

For the short-range potential, $w(r)$, the Bessel function in the integrand can be set to 1. Substituting p_0 and m from Eqs. (6) and (12), we obtain

$$\epsilon_b = \frac{\pi^2 V t_\perp^2}{4c^2} \left[\int d\mathbf{r} w(r) \right]^2. \quad (44)$$

We see that for bilayer graphene, the binding energy is proportional to the gap.[13] The wave function of this localized state not only falls off exponentially with distance, r, from the impurity but also oscillates as $J_0(p_0 r)$. It is clear that when the average distance between the impurities $\sim n_i^{-1/2}$ becomes smaller than p_0^{-1}, the impurity band merges with the conduction (valence) band. Remarkably, the criterion,

$$n_i > p_0^2, \quad (45)$$

also follows from a very different reasoning. Expression (24) for the tail energy, $\tilde{\epsilon}_t$, in the weak-disorder regime can be rewritten as

$$\tilde{\epsilon}_t = \frac{4n_i t_\perp^2}{Vc^2} \left[\int d\mathbf{r} w(r) \right]^2. \quad (46)$$

Comparing Eq. (46) to Eq. (43), we find that the ratio $\tilde{\epsilon}_t / \epsilon_b$ is $\sim n_i/p_0^2$. Thus the condition [Eq. (45)] that neighboring localized states overlap ensures that the impurity band transforms

into the tail of the conduction (valence) band. Note also that in treating the weak-disorder regime we assumed that the correlator of the disorder potential is given by Eq. (1). By making this assumption we already implied that disorder is not due to individual impurities but rather due to fluctuations of impurity concentration, i.e., that the levels [Eq. (43)] are not formed at n_i satisfying the condition [Eq. (45)]. In conclusion, we rewrite, for completeness, the condition of strong disorder in terms of impurity concentration and binding energy of an individual impurity,

$$\frac{V^3}{\epsilon_b t_\perp^2} < \frac{n_i}{\pi^2 p_0^2} < 4.1 \frac{t_\perp}{\epsilon_b}. \tag{47}$$

We see that the smaller the gap, the broader the interval [Eq. (47)].

The role of trigonal distortion. Trigonal distortion becomes important at low bias, where it modifies the bare spectrum of the bilayer [Eq. (5)]. In the literature (see, e.g., Refs. 9 and 35) the strength of distortion is characterized by a dimensionless parameter $v_3 \approx 0.1$, which is a coefficient in front of a cubic term $\propto 4v_3(c^3 p^3/V t_\perp) \cos 3\phi_{\mathbf{p}}$ in the bare spectrum. Then the condition of applicability of our results can be expressed through v_3 in the following way. (i) For a weak disorder, when the tail, ϵ_t, is smaller than the depth, ϵ_m, of the minimum in the bare spectrum, the condition reads $v_3 \lesssim V/t_\perp$. This condition expresses the requirement that the spectral minimum [Eq. (6)] responsible for the formation of a tail is not affected by the cubic term. (ii) For a strong disorder, $\epsilon_t > \epsilon_m$, the minimum in the bare spectrum is irrelevant for the tail states and the corresponding condition on v_3 becomes weaker, namely, $v_3 \lesssim (V/t_\perp)(\epsilon_t/\epsilon_m)^{1/4}$. This condition emerges from the following reasoning. The characteristic momentum, $\tilde{p}_0$, of the tail state is found by equating $\epsilon(\tilde{p}_0)$ to ϵ_t. Then the magnitude of the cubic term at $p = \tilde{p}_0$ should be compared to ϵ_t. This comparison leads to the above condition. Naturally, in the intermediate regime $\epsilon_t \sim \epsilon_m$, both conditions match.

ACKNOWLEDGMENTS

APPENDIX

Similar to Eq. (31), $\nu(\epsilon)$ in the tail is given by

$$\nu(\epsilon) \propto \exp\left(-\frac{1}{2\gamma} \int d\mathbf{r} |\varphi(\mathbf{r})|^4\right), \tag{A1}$$

where the two-component function $\varphi(\mathbf{r})$ satisfies the equation,

$$\hat{H}\varphi(\mathbf{r}) - |\varphi(\mathbf{r})|^2 \varphi(\mathbf{r}) = \epsilon \varphi(\mathbf{r}), \tag{A2}$$

with $\hat{H}$ being the free Hamiltonian with the spectrum [Eq. (12)] and the eigenfunctions [Eq. (13)]. Searching the solution in the form,

$$\varphi(\mathbf{r}) = \int d\mathbf{p} B(\mathbf{p}) \chi_{\mathbf{p}}^+(\mathbf{r}), \tag{A3}$$

we arrive at the following integral equation for $B(\mathbf{p})$:

$$B(\mathbf{p})[\epsilon^+(\mathbf{p}) - \epsilon] = \frac{1}{(2\pi)^2} \int d\mathbf{r}\left(\int \prod_{i=1,2,3} d\mathbf{p}_i B(\mathbf{p}_i)\right)$$
$$\times (\chi_{\mathbf{p}}^{+*} \chi_{\mathbf{p}_1}^+)(\chi_{\mathbf{p}_2}^{+*} \chi_{\mathbf{p}_3}^+). \tag{A4}$$

Assuming that $B(\mathbf{p})$ depends only on the absolute value of $\mathbf{p}$, we easily perform the angular integration in Eq. (A4). Using explicit forms of the wave-function scalar products, we obtain

$$B(\mathbf{p})[\epsilon^+(\mathbf{p}) - \epsilon] = \pi^2 \int dr r\left(\int \prod_{i=1,2,3} d\mathbf{p}_i B(\mathbf{p}_i)\right)$$
$$\times J_2(pr) J_2(p_1 r) J_2(p_2 r) J_2(p_3 r), \tag{A5}$$

where $J_2(x)$ is the Bessel function of the second order. The product of $J_2(p_i r)$ manifests the difference of Eq. (A5) from the corresponding equation in Ref. 28.

The principal step in solving Eq. (A5) is setting all momenta in the right-hand side equal to p_0. Then the integral over r yields $\frac{1}{2}\ln(\epsilon_m/|\epsilon|)$ so that Eq. (A5) reduces to

$$B(\mathbf{p})\left[\frac{(p - p_0)^2}{2m} - \epsilon\right] = 2p_0 \ln\left(\frac{\epsilon_m}{|\epsilon|}\right)\left[\int_0^\infty dp' B(p')\right]^3. \tag{A6}$$

This equation has an obvious solution of the form,

$$B(p) = \frac{\beta}{\frac{(p - p_0)^2}{2m} + |\epsilon|}. \tag{A7}$$

Substituting Eq. (A7) into Eqs. (A3) and (A6), we find for constant β the value,

$$\beta = \frac{1}{2^{1/2}\pi^{3/2}} p_0^{-1/2}\left(\frac{2m}{|\epsilon|}\right)^{-3/4} \ln^{-1/2}\left(\frac{\epsilon_m}{|\epsilon|}\right), \tag{A8}$$

and for $\varphi(r)$ the form,

$$\varphi(r) = 2\pi^2 \beta p_0 \left(\frac{m}{|\epsilon|}\right)^{1/2}\begin{pmatrix} J_2(p_0 r) \\ 0 \end{pmatrix}, \tag{A9}$$

which is valid for $r \lesssim (2m|\epsilon|)^{-1/2}$. Finally, Eq. (25) emerges upon substituting Eq. (A9) into Eq. (A1).

[1] K. S. Novoselov, E. McCann, S. V. Morozov, V. I. Falko, M. I. Katsnelson, U. Zeitler, D. Jiang, F. Schedin, and A. K. Geim, Nat. Phys. **2**, 177 (2006).

[2] R. V. Gorbachev, F. V. Tikhonenko, A. S. Mayorov, D. W. Horsell, and A. K. Savchenko, Phys. Rev. Lett. **98**, 176805 (2007).

[3] S. V. Morozov, K. S. Novoselov, M. I. Katsnelson, F. Schedin, D. C. Elias, J. A. Jaszczak, and A. K. Geim, Phys. Rev. Lett. **100**, 016602 (2008).

[4] E. A. Henriksen, Z. Jiang, L.-C. Tung, M. E. Schwartz, M. Takita, Y.-J. Wang, P. Kim, and H. L. Stormer, Phys. Rev. Lett. **100**, 087403 (2008).

[5] J. Yan, E. A. Henriksen, P. Kim, and A. Pinczuk, Phys. Rev. Lett. **101**, 136804 (2008).

[6] T. Ohta, A. Bostwick, T. Seyller, K. Horn, and E. Rotenberg, Science **313**, 951 (2006).

[7] E. V. Castro, K. S. Novoselov, S. V. Morozov, N. M. R. Peres, J. M. B. Lopes dos Santos, J. Nilsson, F. Guinea, A. K. Geim, and A. H. Castro Neto, Phys. Rev. Lett. **99**, 216802 (2007).

[8] J. B. Oostinga, H. B. Heersche, X. Liu, A. F. Morpurgo, and L. M. K. Vandersypen, Nature Mater. **7**, 151 (2008).

[9] E. McCann and V. I. Fal'ko, Phys. Rev. Lett. **96**, 086805 (2006).

[10] E. McCann, Phys. Rev. B **74**, 161403(R) (2006).

[11] I. Martin, Y. M. Blanter, and A. F. Morpurgo, Phys. Rev. Lett. **100**, 036804 (2008).

[12] T. Stauber, N. M. R. Peres, F. Guinea, and A. H. Castro Neto, Phys. Rev. B **75**, 115425 (2007).

[13] J. Nilsson and A. H. Castro Neto, Phys. Rev. Lett. **98**, 126801 (2007).

[14] H. Min, B. Sahu, S. K. Banerjee, and A. H. MacDonald, Phys. Rev. B **75**, 155115 (2007).

[15] E. J. Nicol and J. P. Carbotte, Phys. Rev. B **77**, 155409 (2008).

[16] J. Nilsson, A. H. Castro Neto, F. Guinea, and N. M. R. Peres, Phys. Rev. B **76**, 165416 (2007).

[17] L. Benfatto, S. G. Sharapov, and J. P. Carbotte, Phys. Rev. B **77**, 125422 (2008).

[18] E. V. Castro, N. M. R. Peres, T. Stauber, and N. A. P. Silva, Phys. Rev. Lett. **100**, 186803 (2008).

[19] F. Guinea, A. H. Castro Neto, and N. M. R. Peres, Phys. Rev. B **73**, 245426 (2006).

[20] B. Sahu, H. Min, A. H. MacDonald, and S. K. Banerjee, Phys. Rev. B **78**, 045404 (2008).

[21] R. Dillenschneider and J. H. Han, Phys. Rev. B **78**, 045401 (2008).

[22] E. V. Castro, N. M. R. Peres, and J. M. B. Lopes dos Santos, Phys. Status Solidi B **244**, 2311 (2007).

[23] B. I. Halperin and M. Lax, Phys. Rev. **148**, 722 (1966).

[24] J. Zittartz and J. S. Langer, Phys. Rev. **148**, 741 (1966).

[25] D. J. Thouless and M. E. Elzain, J. Phys. C **11**, 3425 (1978).

[26] B. I. Halperin, Phys. Rev. **139**, A104 (1965).

[27] M. E. Raikh and Al. L. Efros, JETP Lett. **48**, 220 (1988).

[28] A. G. Galstyan and M. E. Raikh, Phys. Rev. B **58**, 6736 (1998).

[29] A. V. Chaplik and L. I. Magarill, Phys. Rev. Lett. **96**, 126402 (2006).

[30] J. L. Mañes, F. Guinea, and M. A. H. Vozmediano, Phys. Rev. B **75**, 155424 (2007).

[31] S. I. Pekar, *Research in Electron Theory of Crystals*, AEC-TR-5575 Physics (U.S. GPO, Washington, DC, 1963).

[32] E. Brézin and G. Parisi, J. Phys. C **13**, L307 (1980).

[33] A. L. Efros and M. E. Raikh, in *Optical Properties of Mixed Crystals*, edited by R. J. Elliot and I. P. Ipatova (Elsevier Science, Amsterdam, 1998), p. 133.

[34] F. V. Kusmartsev and E. I. Rashba, JETP Lett. **37**, 130 (1983).

[35] J. Nilsson, A. H. Castro Neto, F. Guinea, and N. M. R. Peres, Phys. Rev. B **78**, 045405 (2008).